The Heptameric Prepore of a Staphylococcal α-Hemolysin Mutant in Lipid Bilayers Imaged by Atomic Force Microscopy†

Ye Fang,‡,§ Stephen Cheley,|| Hagan Bayley,|| and Jie Yang*,‡

Department of Physics, University of Vermont, Cook Building, Burlington, Vermont 05405, and Department of Medical Biochemistry & Genetics, Texas A&M University, College Station, Texas 77843-1114

Received March 17, 1997; Revised Manuscript Received May 14, 1997⊗

ABSTRACT: We have used atomic force microscopy to study the oligomeric state of a genetically engineered mutant of staphylococcal α-hemolysin (αHL-H5) that can be arrested as a "prepore" assembly intermediate. AFM images of αHL-H5 on supported bilayers of a fluid-phase lipid, egg-yolk phosphatidylcholine (egg-PC), under conditions that lock αHL-H5 into the prepore state, clearly show a heptameric structure for many individual oligomers. The central dent of the prepore has a diameter of 3.2 ± 0.2 nm. The distance between the centers of mass of neighboring subunits is 2.8 ± 0.3 nm. The heptamer has an average diameter of 8.9 ± 0.6 nm. These results support a recently proposed pathway for the assembly of α-hemolysin.

The staphylococcal α-hemolysin (αHL)[1] membrane pore is formed by the oligomerization of individual subunits after they bind to membranes (Bayley, 1995; Bhakdi & Tranum-Jensen, 1991). Biochemical and crystallographic studies have demonstrated that the pore contains seven subunits (Gouaux et al., 1994; Song et al., 1996). The structure at 1.9 Å of αHL oligomers formed in detergent further shows that each subunit contributes 2 strands (residues 110−148) to a 14-stranded antiparallel *β*-barrel of which the lower part spans the membrane (Song et al., 1996). A molecular switch has been genetically engineered in the membrane-spanning region of αHL by the replacement of 5 residues (130−134) of the 293-residue polypeptide with 5 histidines (αHL-H5) (Walker et al., 1994). The mutant αHL-H5 assembles into a prepore on membranes in the presence of 0.1 mM Zn^{2+} ions at neutral pH. Chelation of Zn^{2+} ions with EDTA allows complete assembly of the membrane pore (the open state). Thereafter, Zn^{2+} ions can block the pore activity. The blocked state is different from either the prepore or the open state. These studies support a model of stepwise assembly for αHL membrane pores (Walker et al., 1992, 1995).

We have now used atomic force microscopy (AFM) as a direct method to investigate the assembly process of αHL-H5 on bilayer membranes. AFM is a useful imaging tool for surface topographical features in solution (Drake et al., 1989), as demonstrated by high-resolution imaging of several classes of biological macromolecules (Fang & Yang, 1997b; Hoh et al., 1993; Karrasch et al., 1994; Mou et al., 1995; Schabert et al., 1995; Shao & Yang, 1995; Yang et al., 1993, 1994). Our results show that αHL-H5 oligomerizes into heptamers on supported bilayers of egg-PC under conditions that ensure assembly cannot proceed beyond the prepore stage. The dimensions of the prepore have been determined from an average of individual images of the heptamer.

MATERIALS AND METHODS

Egg-PC dissolved in chloroform was purchased from Avanti Polar Lipids. Supported bilayers of egg-PC were prepared by the vesicle fusion method (Fang & Yang, 1997a). Briefly, 0.2 mL of vesicular lipid suspension (0.25−0.5 mg/mL in the buffer solution that was used later for incubation with αHL-H5) was applied to freshly cleaved mica and incubated at 4 °C overnight. Then, the substrate, still immersed in the suspension, was heated to 30 °C for about 30 min. To remove excess vesicles, we withdrew 0.15 mL of fluid and replaced it with the same amount of the buffer solution, and repeated the exchange procedure over 20 times. This procedure guaranteed that the specimen remained fully hydrated during the whole process.

A NanoScope E AFM and oxide-sharpened Si_3N_4 tips with a nominal spring constant of 0.06 N/m from Digital Instruments were used. AFM images were obtained in the contact-mode under about 0.1 nN probe force and at a pixel number of 512 × 512. During the AFM scan, any drift in the imaging force was promptly adjusted to keep the imaging force from increasing. All AFM images were obtained in the corresponding incubation buffer. High-quality images were not routinely obtained with all tips used. We often observed round objects without much detail. Typically, several tips were used for each specimen. There were cases in which details of assembled oligomers were not resolved even after more than 10 tips had been used. With a good tip, the specimen could sustain repeated scans without any apparent damage as long as the image force was kept at about 0.1 nN. Most AFM images were obtained at a scanning line speed of 5 Hz.

Image averaging was performed to increase the signal-to-noise ratio. The method was essentially that reported elsewhere (Yang et al., 1994). Briefly, individual oligomers

† Support by the U.S. Army Research Office (J.Y.), the U.S. Department of Energy (H.B.), and the Office of Naval Research (H.B.).

* Corresponding author.

‡ University of Vermont.

§ Present address: Physiology Department, Johns Hopkins University, Baltimore, MD 21205.

|| Texas A&M University.

⊗ Abstract published in *Advance ACS Abstracts,* July 15, 1997.

[1] Abbreviations: αHL, staphylococcal α-hemolysin; αHL-H5, a mutant of αHL in which 5 residues (130−134) of the 293-residue polypeptide have been replaced with 5 histidines; AFM, atomic force microscopy; egg-PC, egg-yolk phosphatidylcholine.

S0006-2960(97)00600-4 CCC: $14.00

were zoomed out from original AFM images so that the center of the oligomer coincided with the center of the zoomed image (size: 13.6 nm). Each oligomer was aligned with respect to a reference chosen from one of the oligomers, by finding the minimum in the χ^2 distance (Frank & van Heel, 1982) between the two images as the first image was rotated in 360 1° steps. The χ^2 distance is defined as

$$D^2[d1, d2(\theta)] = D\sum_{i,j}[D_{d1}(i, j) - D_{d2}(i, j)]^2 \qquad (1)$$

in which D is a normalization constant, $D_{d1}(i, j)$ represents the data at (i, j) of the reference image, and $D_{d2}(i, j)$ represents the data at (i, j) of the oligomer image at a rotation angle θ. Then, the averaged image was used as the reference to realign individual oligomers again, and so forth. We found that the alignment converged after the second average.

The dimensions of the heptamer were determined from an average of 18 heptamers. For the averaged image, a horizontal sectional plot through the center shows a central dent flanked by two maxima. The two maxima are not both at the centers of mass of subunits, because of the heptameric 7-fold symmetry. However, we obtained the diameters of the central dent and the heptamer by averaging the full widths at half-height at the inner and outer edges of the two maxima, repectively. The averaging was carried out by rotating the heptamer in 180 1° steps. Because of the unknown extent of compression as the tip scans the sample, the height of the oligomer obtained from AFM images may not reflect the true dimensions of the molecule. Thus, we have not attempted to obtain molecular dimensions in the vertical direction.

The mutant αHL-H5 was prepared by a modification of the procedure of Walker et al. (1994). *E. coli* JM109 (DE3) (Promega), freshly transformed with pT7Sf1A-H5, was used to inoculate 10 mL of LB/amp (Luria−Bertani medium containing 0.1 mg/mL ampicillin). The cells were grown for 8 h at 37 °C and then used to inoculate 1 L of LB/amp. The cells were grown at 28 °C to an OD_{570} of 2.0 and then recovered by centrifugation at 5000*g* for 20 min. The pellet was resuspended in 10 mL of ice-cold buffer A [50 mM Tris-HCl, 10 mM imidazole, and 150 mM NaCl (pH 8.0)] and then passed through a French press (prechilled on ice) at 8000 psi. The resulting cell lysate was centrifuged at 125000*g* for 60 min at 4 °C and then loaded onto a Ni(II)-NTA (nitrilotriacetic acid)-derivatized agarose column that had been preequilibrated in buffer A 4 °C. The column was washed with 10 bed volumes of buffer A, and bound protein was then released with 8 bed volumes of buffer B [50 mM Tris-HCl, 100 mM imidazole, and 150 mM NaCl (pH 8.0)]. The eluate was dialyzed overnight at 4 °C against 2 L of 10 mM sodium acetate (pH 5.2). Precipitated protein was removed by centrifugation at 14000*g*. The supernatant was loaded onto the strong cation exchange resin [S-Sepharose FF; Pharmacia (10 mL of resin/L of culture)] and eluted with a linear salt gradient (100−300 mM NaCl in 10 mM sodium acetate; pH 5.2), again at 4 °C. Portions were analyzed by SDS−PAGE on a 12% gel. Fractions containing αHL-H5 of >95% purity were pooled, aliqoted, and stored at −70 °C.

Monomeric αHL-H5 subunits were incubated with supported bilayers of egg-PC. Typical incubation times were 5 days to 12 days at room temperature. For some of the samples, we found that the image quality improved after an additional incubation at 37 °C for about an hour, after the long incubation period. It is possible that an increase in the diffusion coefficient at 37 °C facilitates rearrangement of membrane-bound oligomers to make them more closely packed, which helps to allow the specimen withstand the tip disturbance. Solutions used in the incubation included: (1) 0.1 mM $ZnSO_4$, 1 mM MOPS, 20 mM NaCl, pH 7.3; and (2) 0.12 mM $ZnSO_4$, about pH 6.5. Before imaging, excess αHL-H5 subunits were removed by repeated exchange with the incubation buffer to avoid exposing the bilayer to air.

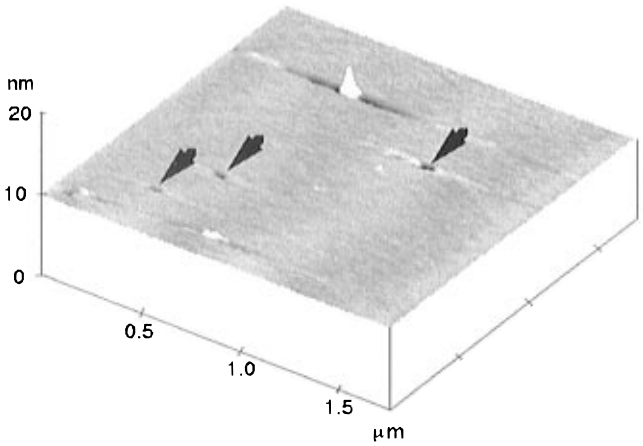

FIGURE 1: Surface plot of a fluid-phase-supported bilayer of egg-PC in 20 mM NaCl. Arrows point to bilayer defects. Some white spots are debris scattered on the bilayer surface.

RESULTS

The use of supported bilayers has allowed in situ high-resolution studies of membrane-bound αHL-H5 with AFM. In our studies, the planar bilayers were of egg-PC and had mixed acyl chains. However, the bilayers were free of any other membrane proteins. Because of the fluidity of these lipids at room temperature, we could not create a large bilayer defect by the scraping method (Fang & Yang, 1996). Small bilayer defects occurring naturally indicated the existence of a supported bilayer but were not suitable for measuring the bilayer thickness (Figure 1). There were also many specimens without any defect within a scanning size of several micrometers. Three to four bilayers were usually prepared in one group. Sometimes there might be one specimen in the group without any bilayer defect. Then, we assumed that the bilayer was present because the other specimens, prepared at the same time, had defects.

By incubating egg-PC bilayers with αHL-H5 subunits for more than 5 days, we observed assembled oligomers on the surface at very high coverage (Figure 2). AFM images of similar quality were also obtained for specimens with an incubation time of 12 days. For specimens with shorter incubation periods (<4 days), we only observed globular structures of about 10 nm in diameter with lower surface coverage, and without any high-resolution details.

To test the effect of the relatively large organic buffer ions, we tried to image in a solution without any MOPS (0.12 mM $ZnSO_4$, about pH 6.5). High-resolution imaging again revealed oligomers on egg-PC membranes (Figure 3). In this case, the probability of achieving stable imaging was higher. The incubation time, however, also required 5 days

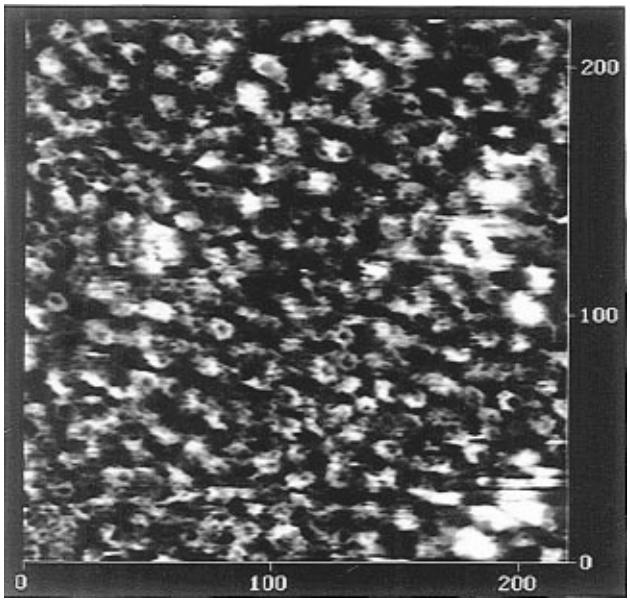

FIGURE 2: AFM image of αHL-H5 on a bilayer of egg-PC in 20 mM NaCl, 0.1 mM $ZnSO_4$, and 1 mM MOPS, pH 7.3. This specimen had an incubation time of 5 days, and the image was taken at a scanning line speed of 5.5 Hz.

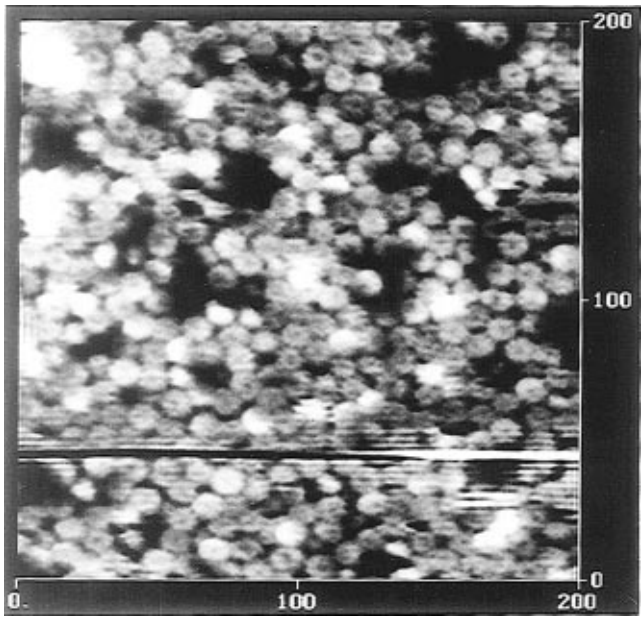

FIGURE 3: AFM image of αHL-H5 on an egg-PC bilayer without large organic ions (0.12 mM $ZnSO_4$, about pH 6.5). The incubation time for this specimen was 7 days, and an incubation at 37 °C for 1 h after the 7-day incubation.

or longer for the surface coverage to be high enough to allow stable high-resolution in situ imaging.

Structural details of the oligomeric prepores visualized by AFM can be seen in Figure 4, in which a gallery of individual oligomers is shown. In this gallery, the images i.a to ii.f were obtained in 1 mM MOPS, 20 mM NaCl, and 0.1 mM $ZnSO_4$, and the images iii.a to iii.e were obtained in 0.12 mM $ZnSO_4$. These images show that the prepore has a heptameric structure, consistent with biochemical studies reported elsewhere (Walker et al., 1995). The image in iii.f is an average of 18 individual oligomers, and shows clearly the heptameric structure of the prepore. From the average map, we determined molecular dimensions of the prepore. The distance between the centers of mass of neighboring

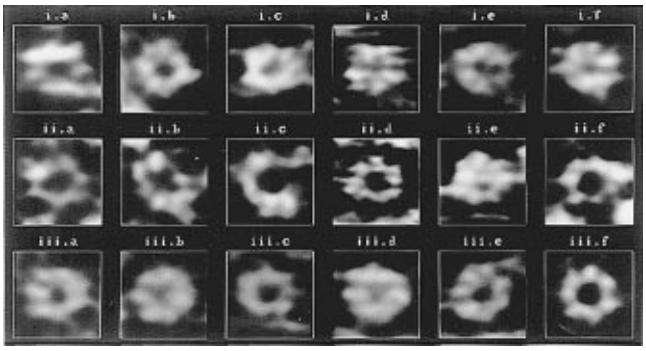

FIGURE 4: Gallery of individual αHL-H5 oligomers in 20 mM NaCl, 0.1 mM $ZnSO_4$, and 1 mM MOPS, pH 7.3 (i.a to ii.f), and in 0.12 mM $ZnSO_4$ (iii.a to iii.e). The image in iii.f is an average of 18 oligomers. Image size: 13.6 nm each.

subunits is 2.8 ± 0.3 nm, consistent with the X-ray studies of the αHL pore (Song et al., 1996). The diameter of the central dent is 3.2 ± 0.2 nm, and the diameter of the prepore is 8.9 ± 0.6 nm.

DISCUSSION

Our results show the power of AFM in high-resolution structural studies of membrane proteins in an aqueous environment. The limit of the new technology lies with the unknown structural characteristics of AFM tips. In our experiments, a large number of tips were used, of which about 10% produced images with well-resolved subunits. Typical Si_3N_4 tips have a radius of curvature of 30−50 nm (Albrecht et al., 1990), and with the oxide-sharpening process, the radius of curvature is still 15−20 nm (Radmacher et al., 1995; Vesenka et al., 1993). If our tips were smooth at their ends, the resolution would have been much lower than that obtained. Nanometer resolution has also been obtained on other biological specimens in which the macromolecules are not ordered into 2-D arrays (Fang & Yang, 1997b; Mou et al., 1995; Yang et al., 1993, 1994). Thus, some AFM tips must contain sharp protrusions that provide the high-resolution images, currently viewed by many researchers (Lyubchenko et al., 1993; Keller, 1996; Yang & Shao, 1993; Yang et al., 1996). While the uncertainty of the structure of these protrusions resulted in the need to use many tips in high-resolution AFM experiments, the resolution obtained is very encouraging. In our case, individual subunits have been directly resolved on many αHL oligomers, indicating an improvement in resolution over conventional electron microscopy (Bhakdi et al., 1981; Olofsson et al., 1988).

Our experiments show that stable AFM imaging essential for high resolution is favored by low ionic strength environments, consistent with experiments reported elsewhere (Fang & Yang, 1997b; Mou et al., 1995). A hydration layer envelops biological macromolecules in solution, and the nature of the hydration force has been extensively studied (Israelachvili & Wennerström, 1996; Leikin et al., 1993; Parsegian, 1973). It appears that hydrated ions may associate with the immediate hydration layer around macromolecules to form a complex hydration layer. The association of the complex hydration layer with macromolecules is stronger at higher ionic strengths (Pashley, 1981). It is possible that the complex hydration layer screens the tip−sample interaction at higher ionic strengths and thereby reduces the image contrast. Larger organic buffer ions associated with the

complex hydration layer may be more susceptible to tip disturbance than smaller ions. This might be the reason that the probability of stable imaging was higher without MOPS. We tried to image in 10 mM MOPS, 0.1 mM $ZnSO_4$, pH 7.4, and the imaging force was always unstable, rendering it impossible to attain stable imaging.

There is evidence that lipids in the lower leaflet of a supported bilayer undergo similar diffusive movements to those in the upper leaflet (Tamm & McConnell, 1985). Thus, fluid-phase-supported bilayers should be suitable substrates for the assembly of αHL-H5. Experiments with other membranes, especially those of red blood cells (RBC), have shown that αHL-H5 is locked in the prepore form in the presence of Zn^{2+} ions (Walker et al., 1995). Additional experiments have shown that Zn^{2+} ions lock αHL-H5 for periods more than a week on both liposomes and RBC. Moreover, the prepore was still functional afterward as pore formation occurred upon the removal of Zn^{2+} ions with the chelating agent EDTA (unpublished results). *In situ* AFM imaging avoids any harsh specimen treatments, such as staining, fixing, or dehydration, and should preserve the structure of the proteins being imaged. Therefore, the observed heptamer in this study must represent the structure of the prepore. Although the assembly of the αHL-H5 prepore on cellular and unsupported lipid membranes takes minutes (Walker et al., 1994, 1995), our studies show that the assembly of αHL-H5 on supported bilayers at high surface coverage is a rather slow process, of the order of days. This slow process is also different from the behavior of wild-type αHL on cellular and vesicular membranes (Bhakdi et al., 1981; Freer et al., 1968; Olofsson et al., 1988). In particular, electron microscopy studies have shown that αHL subunits readily form membrane pores at high density in vesicular phospholipid bilayers (Freer et al., 1968).

The mechanism for this slow process on supported egg-PC bilayers is not understood at present. However, such a slow process on planar bilayers poses a problem for the imaging of the pore form, as opposed to the prepore form, of wild-type α-HL or αHL-H5 (without Zn^{2+} ions). Since the assembly of α-HL on bilayer membranes is stepwise, as demonstrated in earlier biochemical studies (Walker et al., 1995), we cannot be certain that pore formation is completed on supported planar bilayers within the time scale of the experiments. Currently, we are devising independent methods to determine whether the pore can indeed complete assembly on supported planar bilayers. Despite these uncertainties, we did image wild-type α-HL and αHL-H5 without Zn^{2+} ions, and observed similar heptamers (data not shown).

The observation of a heptameric prepore provides direct structural support to earlier biochemical studies (Walker et al., 1995). The dimensions of the prepore are slightly larger than those of the αHL membrane pore viewed from the top of the X-ray structure (2.6 nm diameter pore when viewed from the top, and an average heptameric diameter of about 8.6 nm) (Song et al., 1996). One possibility is that the prepore is slightly larger than the pore, since the amino latch (Ala^1−Val^{20}), that makes extensive contacts with an adjacent protomer in the fully assembled conformation and lines the outer/cis entrance to the pore (Song et al., 1996), is still flexible and susceptible to proteolysis in the prepore form (Walker et al., 1992). In particular, a larger central dent is consistent with the conformational lability of the amino latches in the prepore. It may also be possible that the compression of the oligomer by the AFM tip may enlarge the lateral dimension in addition to a broadening resulting from image-convolution of the tip radius. Moreover, the αHL heptamer viewed from the top of the X-ray structure contains seven closely packed subunits (Song et al., 1996). Some individual heptamers presented in this study show a distinct separation between neighboring subunits. Tip compression may contribute to some of the separation. Given the present limitation of AFM imaging, the dimensions of the prepore cannot be distinguished from those of the fully assembled αHL pore seen in crystals.

In conclusion, we have shown that a genetically engineered αHL assembles into stable heptamers on fluid-phase egg-PC bilayers under conditions that lock the oligomer into the prepore. This result supports the earlier biochemical determination that the prepore is a heptamer (Walker et al., 1995), and shows that the extramembranous part of the structure does not differ dramatically from the fully assembled pore.

ACKNOWLEDGMENT

We thank Christopher Shustak for technical assistance. We thank the reviewers for their helpful comments.

REFERENCES

Albrecht, T. R., Akamine, S., Carver, T. E., & Quate, C. F. (1990) *J. Vac. Sci. Technol. A8*, 3386−3396.
Bayley, H. (1995) *Bioorg. Chem. 23*, 340−354.
Bhakdi, S., & Trannum-Jensen, J. (1991) *Microbiol. Rev. 55*, 733−751.
Bhakdi, S., Füssle, R., & Tranum-Jensen, J. (1981) *Proc. Natl. Acad. Sci. U.S.A. 78*, 5475−5479.
Drake, B., Prater, C. B., Weisenhorn, A. L., Gould, S. A. C., Albrecht, T. R., Quate, C. F., Cannell, D. S., Hansma, H. G., & Hansma, P. K. (1989) *Science 243*, 1586−1589.
Fang, Y., & Yang, J. (1996) *Phys. Chem. 100*, 15614−15619.
Fang, Y., & Yang, J. (1997a) *Biochim. Biophys. Acta 1324*, 309−319.
Fang, Y., & Yang, J. (1997b) *J. Phys. Chem. 101*, 441−449.
Frank, J., & van Heel, M. (1982) *J. Mol. Biol. 161*, 134−137.
Freer, J. H., Arbuthnott, J. P., & Bernheimer, A. W. (1968) *J. Bacteriol. 95*, 1153−1168.
Gennis, R. B. (1994) *Biomembranes, Molecular Structure and Function*, Springer-Verlag, New York.
Gouaux, J. E., Braha, O., Hobaugh, M. R., Song, L., Cheley, S., Shustak, C., & Bayley, H. (1994) *Proc. Natl. Acad. Sci. U.S.A. 91*, 12828−12831.
Hoh, J. H., Sosinsky, G. E., Revel, J.-P., & Hansma, P. K. (1993) *Biophys. J. 65*, 149−163.
Israelachvili, J., & Wennerström, H. (1996) *Nature 379*, 219−225.
Karrasch, S., Hegerl, R., Hoh, J. H., Baumeister, W., & Engel, A. (1994) *Proc. Natl. Acad. Sci. U.S.A. 91*, 836−838.
Keller, D. (1996) *Nature* 384, 111.
Leikin, S., Parsegian, V. A., Rau, D. C., & Rand, R. P. (1993) *Annu. Rev. Phys. Chem. 44*, 369−395.
Lyubchenko, Y. L., Oden, P. I., Lampner, D., Lindsay, S. M., & Dunker, K. A. (1993) *Nucleic Acids Res. 21*, 1117−1123.
Mou, J., Yang, J., & Shao, Z. (1995) *J. Mol. Biol. 248*, 507−512.
Olofsson, A., Kaveus, U., Thelestam, M., & Hebert, H. (1988) *J. Ultrastruct. Mol. Struct. Res. 100*, 194−200.
Parsegian, V. A. (1973) *Annu. Rev. Biophys. Bioeng. 2*, 221−255.
Pashley, R. M. (1981) *J. Colloid Interface Sci. 2*, 531−546.
Radmacher, M., Fritz, M., & Hansma, P. K. (1995) *Biophys. J. 69*, 264−270.
Sackmann, E. (1994) *FEBS Lett. 346*, 3−16.
Shao, Z., & Yang, J. (1995) *Q. Rev. Biophys. 28*, 195−251.
Song, L., Hobaugh, M. R., Shustak, C., Cheley, S., Bayley, H., & Gouaux, J. E. (1996) *Science 274*, 1859−1865.
Tamm, L. K., & McConnell, H. M. (1985) *Biophys. J. 47*, 105−113.

Vesenka, J., Manne, S., Giberson, R., Marsh, T., & Henderson, E. (1993) *Biophys. J. 65*, 992−997.
Walker, B. J., Krishnasastry, M., Zorn, L., & Bayley, H. (1992) *J. Biol. Chem. 267*, 21782−21786.
Walker, B. J., Kasianowicz, J., Krishnasastry, M., & Bayley, H. (1994) *Protein Eng. 7*, 655−662.
Walker, B., Braha, O., Cheley, S., & Bayley, H. (1995) *Chem. Biol. 2*, 99−105.
Yang, J., & Shao, Z. (1993) *Ultramicroscopy 50*, 157−170.
Yang, J., Tamm, L. K., Tillack, T. W., & Shao, Z. (1993) *J. Mol. Biol. 229*, 286−290.
Yang, J., Mou, J., & Shao, Z. (1994) *FEBS Lett. 338*, 89−92.
Yang, J., Mou, J., Yuan, J. Y., & Shao, Z. (1996) *J. Microsc. 182*, 106−113.

BI970600J